Groundwater for Sustainable Development 4 (2017) 12–22

Contents lists available at ScienceDirect

Groundwater for Sustainable Development

journal homepage: www.elsevier.com/locate/gsd

Research paper

Evaluation of potential health risk of heavy metals in groundwater using the integration of indicator kriging and multivariate statistical methods

Lazhar Belkhiri[a,*], Lotfi Mouni[b], Tahoora Sheikhy Narany[c], Ammar Tiri[a]

[a] Laboratory of Applied Research in Hydraulics, University of Batna 2, Algeria
[b] Laboratoire de gestion et valorisation des ressources naturelles et assurance qualité, Faculté des sciences de la nature et de la vie et sciences de la terre, université de Bouira 10000, Algeria
[c] Faculty of Environmental Studies, Universiti Putra Malaysia (UPM), Serdang, 43400 Selangor, Malaysia

ARTICLE INFO

Keywords:
Groundwater
Heavy metals
Multivariate statistical methods
Indicator kriging
Probability map
Human health risk assessment

ABSTRACT

The factors and mechanism which control the spatial patterns of heavy metals in groundwater and their effect on human health could be identified with multivariate statistical methods and human health risk assessment. Sampling wells are statistically classified into two cluster based on the similar characters in groundwater quality using Q-mode cluster analysis (Q-mode CA). Two significant factors were extracted by principal component analyses (PCA), explaining 64.19% of the total variance. These factors were in turn described by the clusters 1 and 2, respectively, resulting from the R-mode CA. PCA and CA revealed significant anthropogenic contributions and water-rock interaction effects of the metals in groundwater. Health risk assessment factors including chronic daily intake (CDI) and hazard quotient (HQ) indices were computed for child and adult. The HQ indices of Cd and Pb in the both child and adult cases showed the value greater than the safe limits, which cause the harmful health hazards and potential non-carcinogenic health risks to the human. Spatial variability maps using ordinary kriging show that safe zones are mainly covered the west and south-western parts of the study area, while the contamination zones are found to be concentrated in the east, north, and south-eastern parts of the plain. The indicator kriging maps show highly uneven spatial pattern of Pb and Cd concentrations. The probability maps reveal that more than 50% of the total area possessed the highest probability (0.8–1.0) of exceeding the threshold values for Cd and Pb.

1. Introduction

Heavy metal (HM) contamination is one the significant health issue in the world, due to indestructibility of metals and their impact on living organism in concentration greater than thresholds. Therefore, human and ecosystem health need to be assess frequently by monitoring the concentration of heavy metals in the environment. Since, heavy metals are not degradable biologically or chemically, they accumulate in limited space or move over long distance. Heavy metals can occur due to natural or anthropogenic sources. Natural sources including the weathering of soils and rocks (Loska and Wiechula, 2003; Yazdi and Behzad, 2009; Mahjoobi et al., 2010), then being transported by air (Giuliano et al., 2007; Zorer et al., 2009) and water (Das and Krishnaswami, 2007; Elmaci et al., 2007; Kar et al., 2008). Anthropogenic activities are other heavy metal sources, which can influence human health by affecting the on vegetation and food chain.

The possibility of incidence of an event which threatened human and ecosystem health and the magnitude of harmful effects over a time periods could be estimated using human health risk assessment methods (Lim et al., 2008). Human could be exposed by heavy metals in three main way, namely direct intake, inhalation and dermal absorption through skin. According to the literature, ingestion and dermal absorption are usual ways for water exposure (USEPA, 1989, 2004; Wu et al., 2009, 2010).

Estimation of spatial patterns of heavy metals contaminations in groundwater is an important stepin the health risk assessment. Geostatistical approaches applied to estimate heavy metals values at unsampled location based on the collected data from sampling station wells (Arslan, 2012). Geostatistics becomes one of the important modelling methods in the studies of sustainability and management in water resources (Baalousha, 2010; Zhou et al., 2011; Arslan, 2012). Kriging is one of the geostatistical interpolation approaches consist of several methods, including indicator kriging, simple kriging, ordinary kriging and co-kriging, which commonly applied in estimating spatial distribution of variables (Lee et al., 2007). Indicator kriging (IK) is an appropriate non-parametric method, which can estimate a conditional

* Corresponding author.
E-mail addresses: belkhiri_laz@yahoo.fr, belkhiri.la@gmail.com (L. Belkhiri).

http://dx.doi.org/10.1016/j.gsd.2016.10.003
Received 23 February 2016; Received in revised form 20 October 2016; Accepted 25 October 2016
Available online 02 November 2016

cumulative distribution function at un-sampled location (Hassan et al., 2011). Therefore, IK model shows the quantified probability of variable exceed or not exceed a particular threshold.

In this study an IK approach was adopted for analyzing the spatial pattern of heavy metals concentration in Ain Azel plain, Algeria. Moreover, various multivariate statistical analysis such as principal component analysis (PCA), R-mod and Q-mod cluster analysis are applied for explanation of huge and complex water quality data in the study area. The information was obtained by statistical analysis can be useful for water resource management (Krishna et al., 2009).

The main aim of the present study is to identify the spatial pattern and the possible sources of heavy metal concentrations in groundwater to assess the impact on human health using the employment of multivariate statistical methods and health risk assessment indices, and geostatistical techniques.

2. Materials and methods

2.1. Characterization of the studied area

Ain Azel plain is placed in the eastern side of Algeria, which lies between latitudes 35°78′1" N and 35°89′4" N, and longitudes 5°40′4" E and 5°65′0" E (Fig. 1). The local weather of the area is semi-arid and the mean of temperature and rainfall is 15.2 °C and 296 mm/year, respectively (Belkhiri, 2013). Most of the population (more than 30,000) are concentrated in the Ain Azel town and the center of the plain, and agriculture is the main economic activity in this area.

Base on the geological map (Fig. 2), several geological formation belong to Triassic, Jurassic, Cretaceous, Miocene and Mio-Plio-Quaternary existed in the study area (Guiraud, 1973; Vila, 1980) (Fig. 2). The Triassic formation is constructed by evaporite rocks, such as gypsum, anhydrite and halite, clay and carbonate minerals (limestone and dolomite). The Jurassic formation is formulated by limestone, dolomite and marl. Clay, marl, limestone and dolomite are formed the Cretaceous formation. The Miocene formation is constituted by limestone, sandstone, dolomite and conglomerate. The Mio-Plio-Quaternary formation shows a heterogeneous continental detrital sedimentation. Exist two poly-metallic mines (lead and zinc) in the study area, the first is Kherzet Youcef in the west (it was abandoned after the disaster of June 2, 1990) and the second is Chaaba el Hamra in the south of the plain. The presence of the mines indicated that the study area is very rich by minerals. The mines belong to a mining district Pb-Zn. They are characterized by simple paragenesis with sphalerite (ZnS), galena (PbS) and marcasite are the major minerals (Boutaleb, 2001).

The aquifer is extended in the alluvial plain of the Mio-Plio-Quaternary and recharge by stream water flows from different reliefs surrounding the depression inter-mountainous of Ain Azel. Large numbers of wells with different depths from 8 to 38 m were constructed in the plain, which mostly apply for drinking and irrigation (Belkhiri, 2013).

2.2. Groundwater sampling and analysis

In Ain Azel plain, around 18 groundwater samples were carried out from Mio-Plio-Quaternary aquifer in March 2008 (Fig. 1), which mainly supply for domestic and agricultural purposes. The groundwater samples were collected after pumping for 10 min and collected using 4 L acid-washed polypropylene containers. Each sample is immediately filtered on site through 0.45 µm filters on acetate cellulose. Then the filtered samples are transferred into 100-cm^3 polyethylene bottles and immediately acidified to pH < 2 by the addition of Merck™ ultrapure nitric acid (5 ml 6N HNO_3). The samples were analyzed for Al, Cd, Cu, Fe, Pb and Zn using standard procedures by (APHA, 2005). The electrical conductivity (EC), pH and the temperature (T) were measured by multi-parameter WTW (P3 MultiLine pH/LF-SET). The heavy metals are specified by Graphite Furnace Atomic Absorption Spectrophotometer (Perkin-Elmer AAnalyst 700) using multi element Perkin-Elmer standard solutions.

2.3. Multivariate Statistical analysis

Multivariate statistical analysis is an appropriate approach for classifying, modelling and interpreting larg data set in environmental monitoring programs and water quality assessment studies (Liu et al., 2003). Initial information about groundwater quality characterization came from the basic statistics and correlation analysis. Moreover, multivariate statistical analysis, including cluster analysis (CA) and principal component analysis (PCA) were applied on the dataset. In water quality studies, it is important to find the interrelationship in huge groundwater dataset and extracted the important factors influencing groundwater quality, which was used to infer the hypothetical sources of heavy metals (Narany et al., 2014). Therefore, principal component analysis was used on groundwater quality dataset, which also useful to minimized the number of variables with a high loading on each component, thereby facilitating the interpretation of PCA results.

Moreover, samples with similar heavy metal contents could be identified and classified based on the cluster analysis (Panda et al., 2006). CA was formulated based on the Ward-algorithmic method, and the Euclidean distance was employed for measuring the distance between clusters of similar metal contents. Q-mode CA was performed to identify clusters of similar sites on the basis of similarities within a class, whereas R-mode CA was used to determine the association of different water quality parameters as well as the sources and processes with which they were associated. All the data were statistically analyzed using the SPSS software (version 17.0 for Windows) and Statistica v10. The maps were prepared using ArcGIS computer package.

2.4. Human health risk assessment

Regarding to health risk assessment, the chronic risk level was determined using chronic daily intake (CDI) indices and hazard quotient (HQ) indices.

The CDI through water ingestion was calculated according to the modified equation from (USEPA, 1992; Chrostowski, 1994):

$$CDI = C * \frac{DI}{BW} \tag{1}$$

where C, DI and BW represent the concentration of HM in water (µg/l), average daily intake rate (2 l/day) and body weight (72 kg), respectively (USEPA, 2005).

The HQ for non-carcinogenic risk can be calculated by the following equation (USEPA, 1999):

$$HQ = \frac{CDI}{RfD} \tag{2}$$

where, based on the USEPA database the oral toxicity reference dose values (RfD) are 7.0E-01, 5.0E-04, 3.7E-02, 3.0E-01, 3.6E-02, 3.0E-01 mg/kg-day for Al, Cd, Cu, Fe, Pb and Zn, respectively (USEPA, 2005).

The scale of chronic risk level (HQ) based on average daily intake (CDI) and reference dose (mg/kg-day) is classified based on the ratio of CDI/RfD indicating≤1 (no risk) if > 1≤5 (low risk), if > 5≤10 (medium risk) and if > 10 (high risk).

2.5. Geostatistical interpolation methods

Geostatistics is a section of applied statistics expand by Matheron (1971), that deals with estimation and modelling of spatial pattern using of regionalized variables, which fall between random variables and completely deterministic variables (Ahmed, 2007). Geostatistical interpolation methods, such as kriging estimate unknown values from

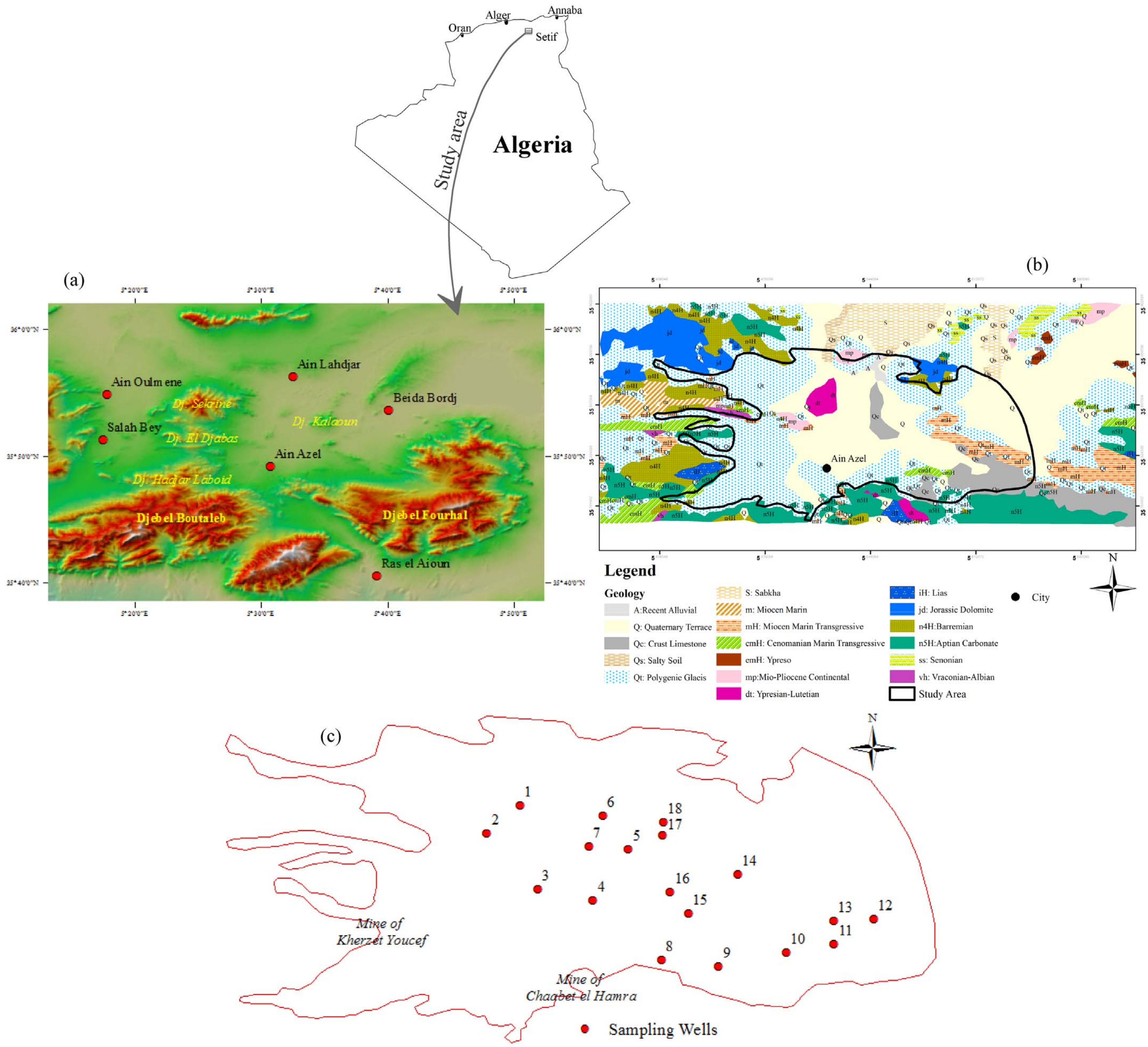

Fig. 1. Location map of the study area (a), Geology map (b) and the sampling wells (c).

data taken at specific locations. Kriging is a best linear unbiased estimator, which can apply to describe and model spatial patterns, predict values at un-sampled location, and assess the uncertainty associated with estimated values at the un-sampled locations (McCoy, 2004).

2.5.1. Ordinary kriging

Ordinary kriging (OK) was applied to interpolate predictive maps of groundwater quality parameters for un-sampled locations. The spatial dependency between nearby observations could be determined with variogram, which is an one-half the variance of the difference between the attribute values at all points separated by h as follows:

$$\hat{\gamma}(h) = \frac{1}{2N(h)}\left\{\sum_{i=1}^{N(h)} [Z(\mu_i + h) - Z(\mu_i)]^2\right\} \quad (3)$$

where, $\hat{\gamma}(h)$ is the variogram for distance h; N(h) represent the number of data pairs for that lag h, and $Z(\mu_i)$ and $Z(\mu_i+h)$ are the values of the regionalized variable of interest at location μ_i and μ_i+h, respectively. In the next step, the computed experimental semivariogram values were fitted in exponential semivariogram model.

2.5.2. Indicator kriging

In the geostatistical techniques, the probability of attribute value is not greater than a specific limitation (Z_k) was estimated using indicator kriging (IK) U (Goovaerts, 2000).

$$I(\mu; Z_k) = \begin{cases} 1 & if \quad Z(\mu) \le Z_k, \quad k = 1, 2, \ldots, m \\ 0 & \quad Otherwise \end{cases} \quad (4)$$

$Z(u)$ is transformed into an indicator variable with binary distribution.

2.5.3. Cross validation

Prediction performances were assessed by cross validation. The measured data are decreased one at time and re-estimated from the rest of data. Observed and estimated values are then compared using standardized mean error (SEM) and root mean square error (RMSE).

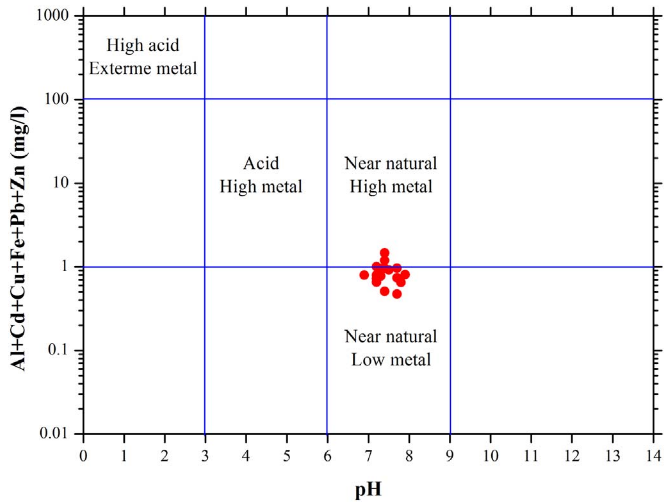

Fig. 2. Scatter diagram of the concentrations of the metals vs. pH.

Table 1
Statistical parameters for selected metal distribution in groundwater.

Parameters	Min	Max	Mean	SD	Cv	Skewness	Kurtosis	WHO
EC	830	2730	1451	557	38.40	1.14	0.46	1500
T	14	18	16	1.4	8.64	−0.41	−1.43	25
pH	6.9	7.9	7.4	0.3	3.47	0.21	−0.24	
Al	10	90	51	22	43.69	0.44	−0.42	30
Cd	9	165	66	45	67.65	0.98	0.19	3
Cu	56	430	241	102	42.25	0.05	−0.27	2000
Fe	55	499	255	116	45.56	0.19	−0.23	300
Pb	17	292	87	69	79.32	1.92	3.92	10
Zn	45	276	148	60	40.47	0.25	0.12	3000

All values are in µg/l except pH, T (°C) and EC (µSiemens/cm).

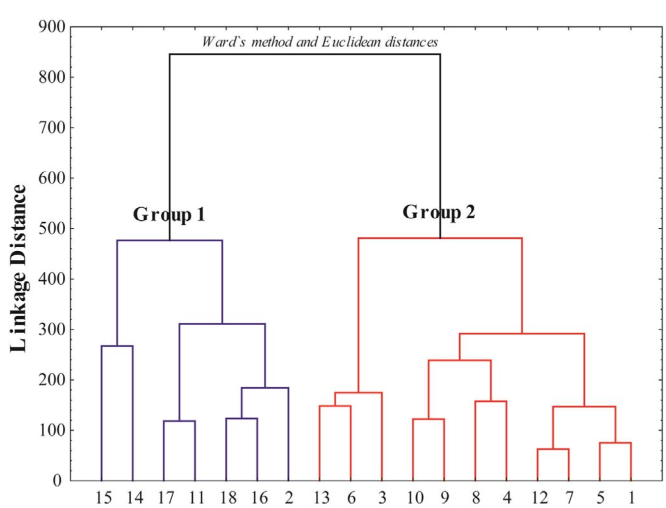

Fig. 3. Q-mod cluster analysis.

Table 2
Mean value of heavy metal in the two groups (µg/l).

Groups	Al	Cd	Cu	Fe	Pb	Zn
Group 1	43	70	185	303	60	133
Group 2	63	61	330	180	129	171

For a model to provide accurate prediction SEM should be close to zero and RMSE should be as small as possible.

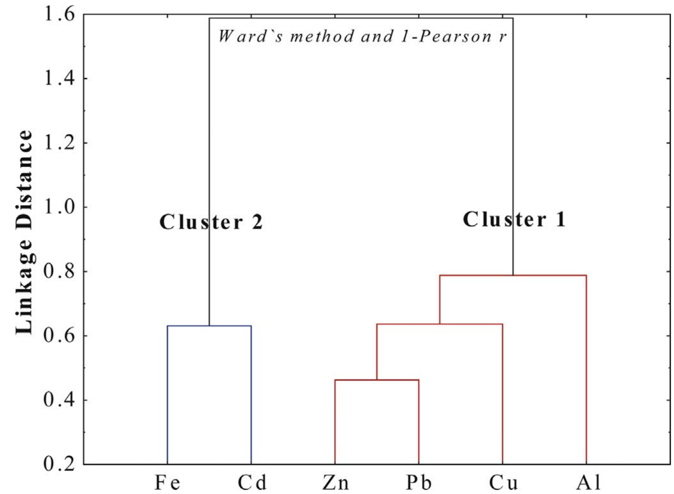

Fig. 4. R-mod cluster analysis.

Table 3
Results of principal component analysis to the heavy metals.

Heavy metals	Factor 1	Factor 2
Al	−0.63	−0.52
Cd	−0.37	0.71
Cu	−0.61	0.05
Fe	0.22	0.86
Pb	−0.85	0.06
Zn	−0.78	0.21
Eigenvalue	2.28	1.57
% Total of variance	38.04	26.16
Cumulative Eigenvalue	2.28	3.85
Cumulative %	38.04	64.19

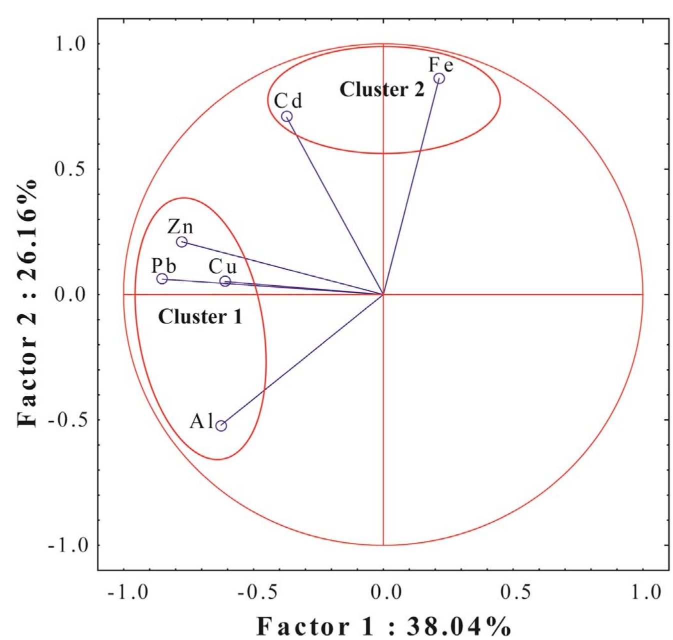

Fig. 5. Projection of the variables on the factor-plane (1×2).

3. Results and discussion

3.1. Groundwater quality

The main descriptive statistics of physicochemical parameters in groundwater were given presented in Table 1. The pH values varied between 6.9 and 7.9 with mean pH of 7.4 for groundwater. All the

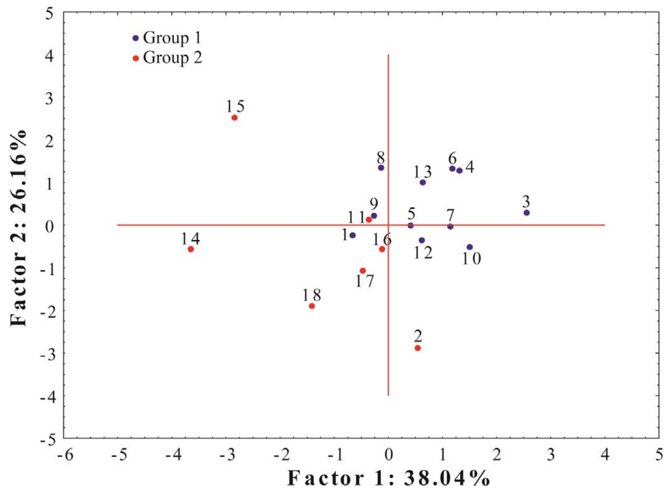

Fig. 6. Projection of the wells on the factor-plane (1×2).

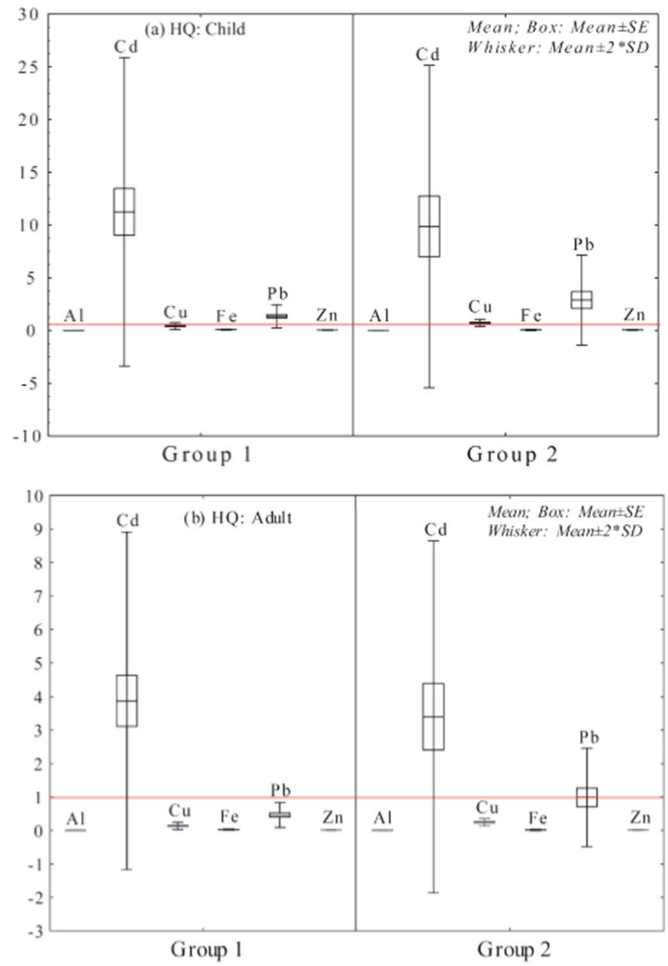

Fig. 7. Box plot of HQ for child (a) and adult (b).

water samples show neutral to slightly alkaline. The temperatures varied from 14 to 18 °C with a mean of 16 °C. All samples show that the values of the temperature were lower than the value fixed by WHO (25 °C) (WHO, 2011). The electrical conductivity (EC) of water is directly proportional to the salinity and could be used as an indicator of ionic concentrations. The EC of groundwater changes between 830 and 2,730 µS/cm with a mean of 1,451 µS/cm, in the study area. The means of Al, Cd, Cu, Fe, Pb, and Zn were 51, 66, 241, 255, 87, and 148 µg/l, respectively (Table 1). Cadmium and lead were found to be above the WHO standard limit (WHO, 2011) in all samples. Most of the samples greater than the desirable limit of Al (83%), but only 39% of them exceeded the desirable limit of Fe (WHO, 2011). Copper and zinc were found to be lower than the maximum permissible limit of WHO standard (WHO, 2011) in all water samples. Based on mean levels in the water samples, the metals followed the decreasing concentration order: Fe > Cu > Zn > Pb > Cd > Al. The metal load was computed as Al +Cd+Cu+Fe+Pb+Zn (mg/l), which showed that around 67% of the water samples plot in the field of near-neutral-low metal, whereas 33% of the samples are characterized as near-neutral-high metal (Fig. 2).

3.2. Spatial similarities and sampling wells grouping

The spatial similarities and wells classification was detected using Q-mod cluster analysis. Samples in the same group contain the similar characteristics respect to the analyzed parameters. Two main groups can be distinguished in the dendrogram shown in Fig. 3. The Table 2 shows that the increases of the most of heavy metals (Al, Cu, Pb and Zn) from the first group to the second group.

The first group was composed of the wells 1, 3, 4, 5, 6, 7, 8, 9, 10, 12, and 13 and concerns 61% of the water samples. The average of electrical conductivity for this group is 1250 µS/cm. In this group concentrations order are Fe > Cu > Zn > Cd > Pb > Al. Group 1 included samples with the highest concentrations of Fe and Cd. The mean concentrations of Fe and Cd are 303 and 70 µg/l, respectively (Table 2).

The second group was represented by the wells 2, 11, 14, 15, 16, 17, and 18, and it occupies 39% of the water samples, where the mean of

Table 4
Chronic daily intake (CDI) indices for heavy metals.

	Group 1					Group 2				
Child	Min	Max	Mean	SD	CV	Min	Max	Mean	SD	CV
Al	0.001	0.006	0.003	0.001	41.986	0.003	0.007	0.005	0.002	37.552
Cd	0.001	0.013	0.006	0.004	64.988	0.001	0.012	0.005	0.004	77.398
Cu	0.005	0.024	0.015	0.006	39.727	0.017	0.035	0.027	0.006	22.596
Fe	0.015	0.040	0.024	0.008	31.247	0.004	0.031	0.015	0.009	62.196
Pb	0.002	0.008	0.005	0.002	40.725	0.001	0.024	0.010	0.008	74.037
Zn	0.004	0.017	0.011	0.004	38.958	0.007	0.022	0.014	0.005	39.729
Adult	Min	Max	Mean	SD	CV	Min	Max	Mean	SD	CV
Al	0.000	0.005	0.002	0.001	64.988	0.000	0.004	0.002	0.001	77.398
Cd	0.002	0.008	0.005	0.002	39.727	0.006	0.012	0.009	0.002	22.596
Cu	0.005	0.014	0.008	0.003	31.247	0.002	0.011	0.005	0.003	62.196
Fe	0.001	0.003	0.002	0.001	40.725	0.000	0.008	0.004	0.003	74.037
Pb	0.001	0.006	0.004	0.001	38.958	0.002	0.008	0.005	0.002	39.729
Zn	0.000	0.002	0.001	0.000	41.986	0.001	0.003	0.002	0.001	37.552

Table 5
Hazard quotient (HQ) indices for heavy metals.

	Group 1				Group 2			
Child	Min	Max	Mean	SD	Min	Max	Mean	SD
Al	0.001	0.008	0.005	0.002	0.005	0.010	0.007	0.003
Cd	2.583	26.637	11.256	7.315	1.453	24.538	9.871	7.640
Cu	0.122	0.657	0.404	0.160	0.465	0.938	0.719	0.162
Fe	0.051	0.134	0.082	0.025	0.015	0.102	0.048	0.030
Pb	0.388	6.547	1.768	1.668	0.000	4.327	1.925	1.635
Zn	0.012	0.056	0.036	0.014	0.012	0.074	0.021	0.018
Adult	Min	Max	Mean	SD	Min	Max	Mean	SD
Al	0.000	0.004	0.002	0.001	0.002	0.004	0.003	0.001
Cd	0.889	9.167	3.873	2.517	0.500	8.440	3.396	2.629
Cu	0.042	0.226	0.139	0.055	0.159	0.323	0.247	0.056
Fe	0.017	0.046	0.028	0.008	0.005	0.035	0.017	0.010
Pb	0.208	0.779	0.463	0.189	0.133	2.253	0.992	0.735
Zn	0.004	0.019	0.012	0.005	0.008	0.025	0.015	0.006

EC is 1766 µS/cm. The mean heavy metals in this group followed a descending order as: Cu > Fe > Zn > Pb > Al > Cd. The water samples of this group characterized by high concentrations of Cu, Zn, Pb and Al. The mean values of Cu, Zn, Pb and Al are 330, 171, 129 and 63 µg/l, respectively (Table 2).

3.3. Heavy metals grouping

R-mod cluster analysis was also performed to visualize heavy metals grouping in the groundwater dataset, and the results are shown in Fig. 4 as a dendrogram. Fig. 4 displays two clusters: (1) Cu-Zn-Pb-Al; (2) Fe-Cd. The concentrations of Cu, Zn, Pb and Al are increased from the first group to the second group and the highest values are observed in the center of the plain with higher intensity of population. Fe and Cd concentrations are decreased from group 1 to group 2 and the high concentrations are observed around the plain and near to the mountains.

3.4. Principal component analysis (PCA)

The source of the heavy metals can be identified using the PCA. The important factors which influenced groundwater quality and the percentage of the variance were calculated by the extracting the

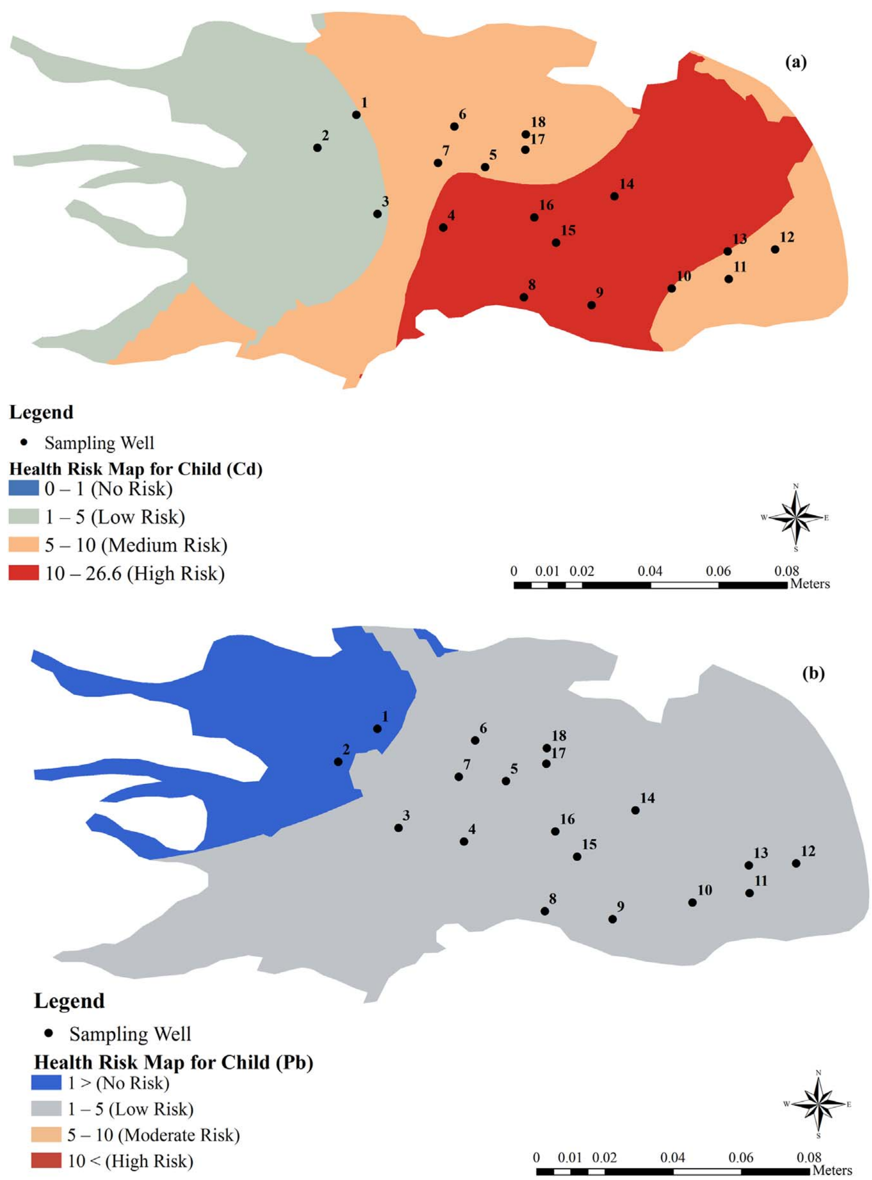

Fig. 8. Spatial distribution map of health risk for cadmium (a) and lead (b) in child case.

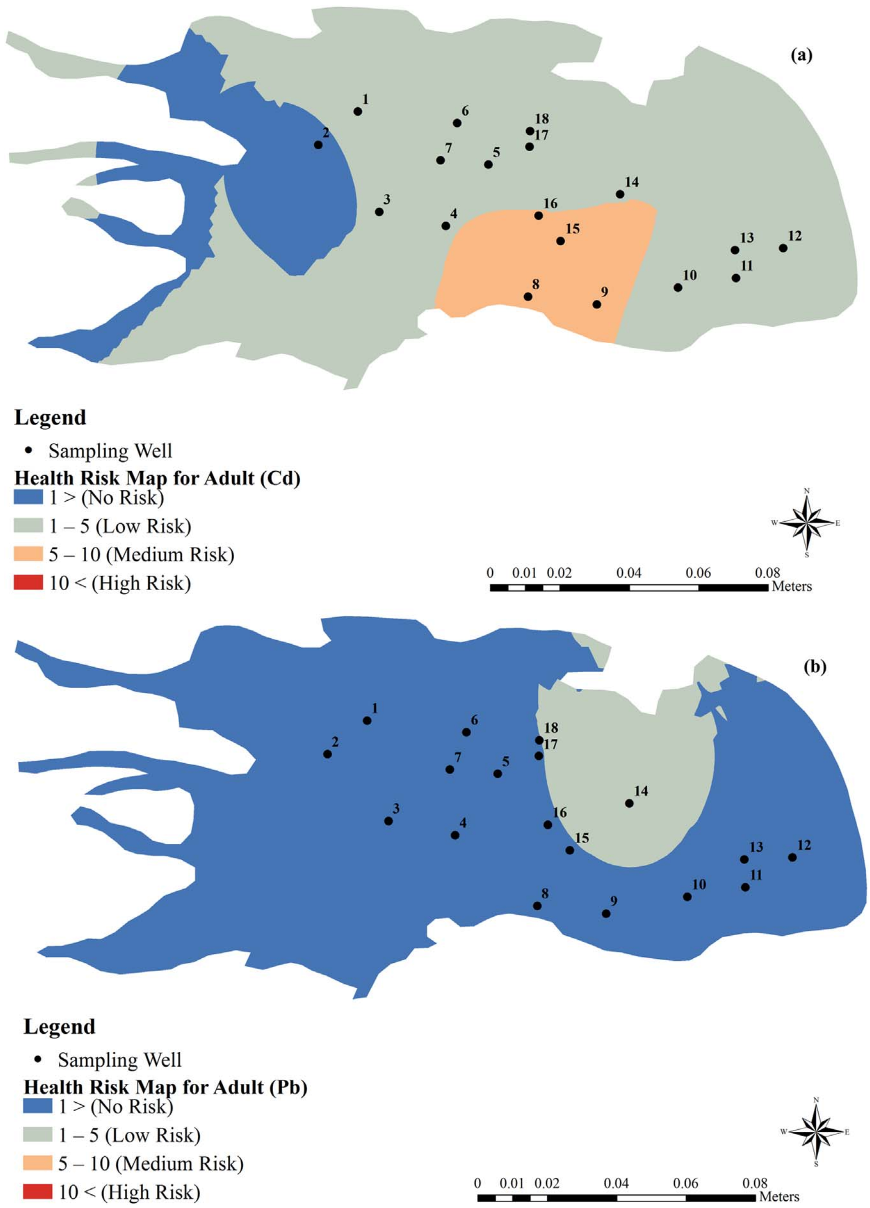

Fig. 9. Spatial distribution map of health risk for cadmium (a) and lead (b) in adult case.

eigenvalues and eigenvectors from the correlation matrix.

The results indicate that there were two eigenvalues higher than one and that these two factors explain 64.19% of the total variance (Table 3). The first factor explains 38.04% of the total variance and loads heavily on Pb, Zn, Al and Cu, supported by cluster 1 (Figs. 5 and 6). This result can be supported by the existence of two polymetallic mines, namely Kherzet Youcef and Chaaba el Hamra in the study area. These metals were mainly contributed by natural sources and agricultural activities. Factor 2 exhibited higher loadings of Fe and Cd, accounts for 26.16% of the total variance, duly supported by cluster 2 (Figs. 5 and 6). These metals were predominantly contributed by natural sources. PCA confirmed and completed the results obtained by CA. Overall, PCA and CA demonstrated significant natural sources and anthropogenic contributions of the heavy metals in groundwater.

3.5. Human health risk assessment

The basic information about the age, food habit, body weight and health problem of local people in the study area was collected during the study, which clearly indicate that the groundwater used as drinking water by the local people. Therefore, health risk assessment like chronic daily intake (CDI) and hazard quotient (HQ) were also calculated to evaluate the impact of heavy metals on human health in the study area.

3.5.1. Chronic daily intake (CDI) indices

The results of CDI values are summarized in Table 4. The CDI values in the first group water changed from 0.001 to 0.006 for Al, 0.001–0.013 for Cd, 0.005–0.024 for Cu, 0.015–0.040 for Fe, 0.002–0.008 for Pb and 0.004–0.017 mg/kg-day for Zn for child. Whereas, for adult CDI values were ranging from 0.000 to 0.005 for Al, 0.002–0.008 for Cd, 0.005–0.014 for Cu, 0.001–0.003 for Fe, 0.001–0.006 for Pb and 0.000–0.002 mg/kg-day for Zn, respectively. Therefore, the toxicity of HM mean concentrations in the group 1 for child and adult were found in the order of Fe > Cu > Zn > Cd > Pb > Al and Cu > Cd > Pb > Fe=Al > Zn, respectively. The high CDI values in child may be attributed to the stage of health risk on human health. Similarly, the CDI values in the second group water used for drinking purpose ranged from 0.003 to 0.007, 0.001–0.012, 0.017–0.035, 0.004–0.031, 0.001–0.024 and 0.007–0.022 mg/kg-day for Al, Cd, Cu, Fe, Pb and Zn for

Table 6
Cross-validation results for ordinary kriging method.

Models	Cir	Sph	Tet	Pen	Exp	Gau	Qua	Hol	K- Bes	J- Bes	Sta
Cd- child case											
ME	0.45	0.47	0.38	0.37	0.19	0.56	0.41	0.48	0.34	0.55	0.37
MSE	0.05	0.06	0.04	0.04	0.02	0.05	0.04	0.06	0.03	0.08	0.04
RMSSE	1.00	0.95	0.94	0.94	0.85	1.11	0.96	1.14	0.94	1.12	0.95
RMSE	4.99	4.94	4.93	4.97	5.12	4.84	5.01	5.11	4.99	5.08	4.96
ASE	5.28	5.38	5.40	5.42	6.04	4.81	5.49	4.66	5.46	4.68	5.41
Pb- child case											
ME	0.00	0.07	0.07	0.05	0.05	0.00	0.03	0.04	0.00	0.05	0.00
MSE	0.00	0.05	0.05	0.04	0.03	0.01	0.02	0.04	0.01	0.05	0.01
RMSSE	0.95	1.00	1.00	0.99	1.00	0.97	0.96	0.96	0.96	0.97	0.97
RMSE	1.41	1.48	1.49	1.48	1.50	1.40	1.49	1.42	1.41	1.43	1.40
ASE	1.44	1.44	1.45	1.45	1.47	1.40	1.52	1.44	1.42	1.42	1.40
Cd- adult case											
ME	0.16	0.16	0.17	0.15	0.17	0.20	0.16	0.30	0.18	0.27	0.20
MSE	0.04	0.04	0.04	0.05	0.04	0.00	0.02	0.01	0.00	0.00	0.00
RMSSE	0.69	0.68	0.68	0.68	0.85	0.86	0.74	0.91	0.90	0.90	0.86
RMSE	1.73	1.70	1.72	1.72	1.76	1.65	1.66	1.69	1.65	1.68	1.65
ASE	2.88	2.91	2.91	2.91	2.88	2.66	2.86	2.60	2.66	2.64	2.66
Pb- adult case											
ME	0.03	0.02	0.02	0.02	0.02	0.07	0.01	0.01	0.01	0.02	0.02
MSE	0.01	0.01	0.01	0.01	0.01	0.01	0.02	0.00	0.01	0.00	0.01
RMSSE	0.80	0.81	0.81	0.82	0.82	0.85	0.80	0.85	0.85	0.84	0.85
RMSE	0.49	0.49	0.49	0.49	0.50	0.48	0.50	0.46	0.48	0.46	0.46
ASE	0.57	0.57	0.57	0.57	0.57	0.54	0.52	0.53	0.54	0.54	0.54

Cir: circular; Sph: spherical; Tet: tetra-spherical; Pen: penta-spherical; Exp: exponential; Gau: gaussian; Qua: quadratic;
Hol: hole-effect; K-Bes: K- Bessel; J-Bes: J- Bessel; Sta: stable.
ME: mean error; MSE: mean standardized error; RMSSE: root mean squared standardized error; RMSE: root mean square error;
ASE: average standardized error.

Table 7
Best-fitted variogram models of factor scores one and two.

Hazard quotient (HQ) indices	Variogram	Nugget (C_0)	Sill (C_0+C)	(C_0/C_0+C)*100
Cd (child case)	Gaussian	4.2782	66.374	6.4%
Pb (child case)	Gaussian	0.94073	2.0845	45.1%
Cd (adult case)	K-Bessel	0.14453	0.74978	19.2%
Pb (adult case)	K-Bessel	0.29120	0.58936	49%

child. Whereas, in the case of adult the CDI values fluctuated from 0.000 to 0.004, 0.006–0.012, 0.002–0.011, 0.000–0.008 and 0.001–0.003 mg/kg-day for Al, Cd, Cu, Fe, Pb and Zn respectively (Table 4). The order of toxicity for both child and adult was found in the order of Cu > Fe > Zn > Pb > Cd=Al and Cd > Cu=Pb > Fe > Zn=Al, respectively.

3.5.2. Hazard quotient (HQ) indices

The mean HQ index values for Al, Cd, Cu, Fe, Pb, and Zn in the first group of water samples for child were 0.005, 11.256, 0.404, 0.082, 1.768, and 0.036, while that of adults were 0.002, 3.873, 0.139, 0.028, 0.463, and 0.012, respectively. Similarly, in the second group of water samples the mean HQ index values were 0.007, 9.871, 0.719, 0.048, 1.925, and 0.021 for child and 0.003, 3.396, 0.247, 0.017, 0.992, and 0.015 for adult, respectively. Therefore, the toxicity of HM mean concentrations for both child and adult in first and second group were found in order, Cd > Pb > Cu > Fe > Zn > Al (Fig. 7a, b).

Table 5 presented HQ risk value for the groups relating to adult and child, respectively. Accordingly, the human health risk assessment of Al, Cu, Fe, and Zn showed HQ values suggesting an acceptable level of non-carcinogenic adverse health risk in most samples of the two groups. However, in contrast, note that Cd and Pb showed HQ values indicating an unacceptable non-carcinogenic health risk. Cd and Pb show risk value (HQ) > 1.0 indicates the potential of an adverse effect to human health and need for more strict control of use. Usage of drinking water contain of lead in greater values rather than the limited standard could be cause of delays in physical and mental development in in six-year-old children or under (USEPA, 2011).

In the case of child, an HQ value of Cd varies from 2.583 to 26.637 and 1.453–24.538 in first and second groups, respectively. Based Fig. 8a, HQ of Cd in all sampling wells of the both groups, were higher than 1, implying that Cd may cause adverse health and non-carcinogenic health risks to the children. Similar to child, HQ of Cd varies from 0.889 to 9.167 in first group and 0.5–8.440 in the second group, for adult, which were higher than 1, in 94.5% of sampling wells. Based on the cadmium health risk distribution maps in the child and adult cases (Figs. 8a and 9a), high risk of cadmium could be observed in the southern region (Dj. Fourhal and mine of Chaaba el Hamra) and eastern region (mine of Kherzet Youcef), which might be principally caused by natural deposits. Cd concentrations are also remarkably higher than maximum threshold (5ppb) (USEPA, 2011), which has the potential to cause kidney, liver, and bone damages in long-term usages in drinking water. The HQ indices for cadmium decreased gradually toward western region. Moreover, HQ indices of Pb varied from 0.388 to 6.547 in the first group, and from 0 to 4.327 in the second group in the child case and varied from 0.208 to 0.779 in the first and from 0.133 to 2.253 in the second group in the adult case. Around 70% of sampling wells in the child case (first and second groups) and around 60% of sampling wells in the adult case (the second group) showed unacceptable non-carcinogenic health risk level for Pb. However, in contrast, all the sampling wells belong to the first group in adult case had no significant non-carcinogenic health risk from Pb. The HQ maps of Pb for the child and adult cases showed that HQ indices of Pb mainly increase from eastern region (mine of Kherzet Youcef) to central of plain (Figs. 8b and 9b), which might be caused by both anthropogenic activities and erosion of natural deposits, such as metalliferous and gangue minerals (Belkhiri et al., 2010, 2011). Therefore, the current study has indicated the necessity of developed precaution to Pb exposure during critical periods in children's development, because

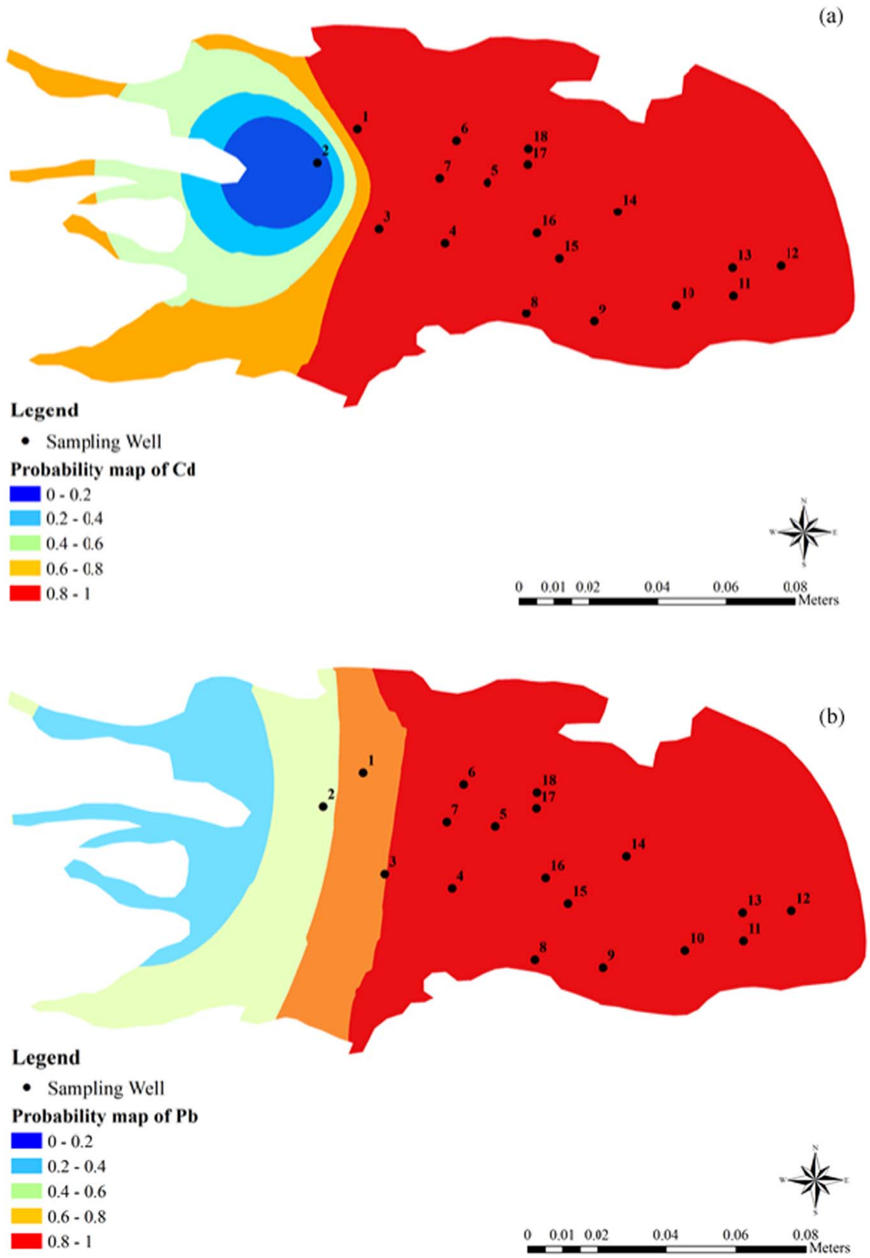

Fig. 10. Probability map of Cd (a) and Pb (b) concentration in the study area.

Table 8
Cross-validation and semivariogram model parameters for probability map of heavy metals concentration.

Parameters	Model	ME	RMSS	Nugget	Sill	Nugget-sill ratio
Pb	Spherical	0.007	1.343	0.0169	0.0757	22.4%
Cd	Spherical	0.006	1.151	0.0227	0.3163	4.9%

of long term health and arising from intrauterine to childhood exposure Pb, often underactable at first only to manifest later in life.

HQ indices of four metals (Fe, Al, Cu, and Zn) for the adult and child cases in the both group was below unity, which revealed the metals do not have any adverse effect and non-carcinogenic health risk.

The results of geostatistical interpolation techniques show that the Gaussian and K-Bessel models was found as the most accurate model for Cd, Pb in child and adult cases, respectively (Table 6). Based on the nugget-sill ratio, the percentage of the overall variance at a distance smaller than the smallest lag interval, and represent the variance in the model. If the ratio is less than 25%, the variable had strong spatial dependence; if the ratio is between 25% and 75%, the variable has moderate spatial dependence; and if greater than 75% the variable show weak spatial dependence (Ahmadi and Sedghamiz, 2007). The nugget-sill ratio indicates that HQ for Cd (in child and adult cases) show strong spatial dependence and Pb (in child and adult cases) show moderate spatial dependency (Table 7).

3.6. *Heavy metals probability map*

Indicator kriging used to generate groundwater probability map for Cd and Pb as a significant heavy metals contaminant which effect child and adult health in the study area. At each sampling well, measurements were subjected to a continuous scale and converted to discrete indicator variables with a value of either “1” or “0” (Sheikhy Narany et al., 2013). Probability maps for Cd and Pb are shown in Fig. 10, and best fit variogram models, cross validation, and nugget-sill ratio of heavy metals are given in Table 8, respectively. Finding from nugget-sill ratio in the present study indicated groundwater heavy metals to have a strong spatial structure, because of all four heavy metals parameters show nugget-sill ratio $< 25\%$ (Table 8). Gaussian model was chosen as a best fitted model using cross validation.

Cadmium concentrations varied from 9 μg/L to 165 μg/L, with the mean value 66 μg/L, which are higher than permissible value (5 μg/L by USEPA (2011) and 3 μg/L by WHO (2011)). Based on the probability map of cadmium concentration (Fig. 10a), more than 55% of the study area (mainly in eastern, northern, and south-eastern sides) showed very strong probability (0.8–1.0) of exceeding the threshold value for Cd. Regarding to the HQ indices results, these areas showed high risk of cadmium concentration for child and adult. Based on the Fig. 10a, probability of exceeding the threshold value for Cd decreased gradually toward western side, where 10.4% of the area showed very weak probability (0.0–0.2).

Lead concentration varied from 17 μg/L to 292 μg/L, with the mean value 87 μg/L. Since the majority of sampling wells show lead concentration higher than 10 μg/L (WHO, 2011), which was used as the threshold value for human consumption, around 62% of the area showed highest probability (0.8–1.0) of exceeding the threshold value for Pb. The high predicted probabilities are located mainly in the east, north-east and south-east region, which was identified as areas with high HQ indices, especially for child (Fig. 10b). More than 18% and 20% of area showed strong probability (0.6–0.8) and moderate probability (0.4–0.6) of exceeding threshold, respectively. Based on the Fig. 10b, the problem of excess lead concentration mainly decreased in west, south-west, and north-west sides of the study area.

4. Conclusion

In this study, multidisciplinary approach, including multivariate statistical methods, health risk assessment, and geostatistics were used to determine the main factors and mechanisms controlling the spatial variation of heavy metals in groundwater and to assess the adverse health effects on the population. Based on the multivariate statistical analysis, two major groups were determined using Q-mod CA. the first group represents 61% of the water samples with the highest concentrations of Fe and Cd and the second group occupies 39% of the water samples and characterized by high concentrations of Cu, Zn, Pb and Al. Two clusters were defined by R-mode CA: (1) Cu-Zn-Pb-Al; (2) Fe-Cd. PCA identified two factors responsible for data structure explaining 64.19%of total variance. The first factor explains 38.04% of the total variance and loads heavily on Pb, Zn, Al and Cu, supported by cluster 1. Factor 2 exhibited higher loadings of Fe and Cd, accounts for 26.16% of the total variance, duly supported by cluster 2. PCA and CA revealed significant anthropogenic contributions and water-rock interaction effects of the metals in groundwater. Human health risk could be threatened by existence of heavy metals in drinking water. The results of health risk assessment in the groundwater of study area indicated that Cd and Pb had HQ > 1which were the main pollutants in the case of child and adult, and could cause adverse health hazards and potential non-carcinogenic health risks to the local people. Application of indicator kriging methods revealed that the majority of plain (more than 55%) face to very strong probability of Pb and Cd concentration exceeding threshold values, which threated human specially child health in the study area. Area with strong probability of heavy metal concentrations need to be monitored strongly to prevent human health hazard.

References

Ahmed, S., 2007. Application of Geostatistics in Hydrosciences. In: Thangarajan, M. (Ed.), Groundwater 321. Springer, Netherlands, 78–111.
Ahmadi, S.H., Sedghamiz, A., 2007. Geostatistical analysis of spatial and temporal variations of groundwater level. Environmental Monitoring and Assessment 129 (1–3), 277–294.
APHA, 2005. Standard Methods for the Examination of Water and Wastewater 19th ed.. American Public Health Association, Washington, DC, 1–467.
Arslan, H., 2012. Spatial and temporal mapping of groundwater salinity using ordinary kriging and indicator kriging: the case of Bafra Plain, Turkey. Agric. Water Manag. 113, 57–63.
Baalousha, H., 2010. Assessment of a groundwater quality monitoring network using vulnerability mapping and geostatistics: a case study from Heretaunga Plains, New Zealand. Agric. Water Manag. 97 (2), 240–246.
L., Belkhiri, A., Boudoukha, L., Mouni, T., Baouz, 2010. Application of multivariate statistical methods and inverse geochemical modeling for characterization of groundwater" A case study: Ain Azel plain (Algeria). Geoderma.159, 3–4, pp. 390-398.
Belkhiri, L., Boudoukha, A., Mouni, L., Baouz, T., 2011. Statistical categorization geochemical modeling of groundwater in Ain Azel plain (Algeria). J. Afr. Earth Sci. 59, 140–148.
L., Belkhiri, A., Boudoukha, 2013. Hydrogéochimie des eaux souterraines. Éditions Universitaires Européenes. pp. 136.
Boutaleb, A., 2001. Mineralizations with Pb-Zn of the Sétifien-Hodna field: Gitology, petrography of dolomites, microthermometry and implications metallogenic. Ph.D. Thesis statement in mining geology, IST. USTHB, Algeria, 260.
Chrostowski, P.C., 1994. Exposure assessment principles. In: Patrick, D.R. (Ed.), Toxic Air Pollution Handbook. Van Nostrand Reinhold, New York, 133–163.
Das, A., Krishnaswami, S., 2007. Elemental geochemistry of river sediments from the Deccan Traps, India: implications to sources of elements and their mobility during basalt–water interaction. Chem Geol. 242 (1-2), 232–254.
Elmaci, A., Teksoy, A., Topac, F., Ozengin, N., Kurtoglu, S., Baskaya, S., 2007. Assessment of heavy metals in Lake Uluabat, Turkey. Afr J Biotechnol 6 (19), 2236–2244.
Goovaerts, P., 2000. Geostatistical approaches for incorporating elevation into the spatial interpolation of rainfall. Journal of hydrology 228 (1), 113–129.
Hassan, M.M., Atkins, P.J., 2011. Application of geostatistics with indicator Kriging for analyzing spatial variability of groundwater arsenic concentrations in Southwest Bangladesh. J. Environ. Sci. Health Part A 46 (11), 1185–1196.
Guiraud, R., 1973. Post-triassic Evolution of before Country of the Alpine Chain of Algeria, According to the Study of the El Eulma Basin and Close Areas, Thesis Natural Sciences, Nice, France, France, pp. 270.
Kar, D., Sur, P., Mandal, S., Saha, T., Kole, R., 2008. Assessment of heavy metal pollution in surface water. Int. J. Environ. Sci. Technol. 5 (1), 119–124.
Krishna, A.K., Satyanarayanan, M., Govil, P.K., 2009. Assessment of heavy metal pollution in water using multivariate statistical techniques in an industrial area: a case study from Patancheru, Medak District, Andhra Pradesh, India. J. Hazard. Mater. 167 (1), 366–373.
Lee, J.J., Jang, C.S., Wang, S.W., Liu, C.W., 2007. Evaluation of potential health risk of arsenic-affected groundwater using indicator kriging and dose response model. Sci. Total Environ. 384 (1), 151–162.
Lim, H.S., Lee, J.S., Chon, H.T., Sager, M., 2008. Heavy metal contamination and health risk assessment in the vicinity of the abandoned Songcheon Au–Ag mine in Korea. J. Geochem. Explor. 96, 223–230.
Liu, W.X., Li, X.D., Shen, Z.G., Wang, D.C., Wai, O.W.H., Li, Y.S., 2003. Multivariate statistical study of heavy metal enrichment in sediments of the Pearl River Estuary. Environ. Pollut. 121, 377–388.
Loska, K., Wiechuła, D., 2003. Application of principal component analysis for the estimation of source of heavy metal contamination in surface sediments from the Rybnik Reservoir. Chemosphere 51 (8), 723–733.
Mahjoobi, A., Albaji, M., Torfi, K., 2010. Determination of heavy metal levels of Kondok soils Haftgel. Res. J. Environ. Sci. 4 (3), 294–299.
Matheron, G., 1971. The theory of regionalized variables and its applications. Ecole nationale supérieure des mines de Paris 5.
McCoy, J., 2004. ArcGIS 9: Using ArcGIS Spatial Analyst. Esri Press.
Narany, T.S., Ramli, M.F., Aris, A.Z., Sulaiman, W.N.A., Fakharian, K., 2014. Spatiotemporal variation of groundwater quality using integrated multivariate statistical and geostatistical approaches in Amol–Babol Plain, Iran. Environ. Monit. Assess. 186 (9), 5797–5815.
Panda, U.C., Sundaray, S.K., Rath, P., Nayak, B.B., Bhatta, D., 2006. Application of factor and cluster analysis for characterization of river and estuarine water systems—a case study: Mahanadi Rive (India). J. Hydrol. 331, 434–445.
Sheikhy Narany, T., Ramli, M.F., Aris, A.Z., Sulaiman, W.N.A., Fakharian, K., 2013. Spatial assessment of groundwater quality monitoring wells using indicator Kriging and risk mapping, Amol-Babol Plain, Iran. Water 6 (1), 68–85.
USEPA (US Environmental Protection Agency), 1989. Risk Assessment Guidance for Superfund, vol. I: Human Health Evaluation Manual (Part A). US Environmental Protection Agency, Office of Emergency and Remedial Response, EPA 540/1-89/002, Washington, DC.
USEPA (US Environmental Protection Agency), 1992. Guidelines for Exposure Assessment, EPA/600/Z-92/001, Risk Assessment Forum, Washington, DC.
USEPA (US Environmental Protection Agency), 1999. Guidance for Performing Aggregate Exposure and Risk Assessments, Office of Pesticide Programs, Washington, DC.
USEPA (US Environmental Protection Agency), 2004. Risk Assessment Guidance for Superfund Volume 1. Human Health Evaluation Manual (Part E, Supplemental Guidance for Dermal Risk Assessment). EPA/540/R/99/005 Office of Superfund Remediation and Technology Innovation; Washington, DC.
USEPA (US Environmental Protection Agency), 2005. Guidelines for Carcinogen Risk Assessment, EPA/630/P-03/001F, Risk Assessment Forum, Washington, DC.
USEPA, 2011. Drinking Water Standards and Health Advisories. Environmental Protection Agency Office of Water U.S., Washington, DC.
Vila, J.M., 1980. The Alpine chain of Eastern Algeria and the Algerian-Tunisian border,

Thesis of doctorate Natural Sciences, Paris VI, France, 665.
WHO (World Health Organization), 2011. Guidelines for Drinking-water Quality. vol 4, 3rd edn. Geneva.
Wu, B., Zhao, D.Y., Jia, H.Y., Zhang, Y., Zhang, X.X., Cheng, S.P., 2009. Preliminary risk assessment of trace metal pollution in surface water from Yangtze River in Nanjing Section, China. Bull. Environ. Contam. Toxicol. 82, 405–409.
Wu, B., Zhang, Y., Zhang, X., Cheng, S., 2010. Health risk from exposure of organic pollutants through drinking water consumption in Nanjing, China. Bull. Environ. Contam. Toxicol. 84, 46–50.
Yazdi, M., Behzad, N., 2009. Heavy metals contamination and distribution in the parks city of Islam Shahr, SW Tehran, Iran. Open Environ. Pollut. Toxicol. J. 1, 49–53.
Zhou, Z.M., Zhang, G.H., Wang, J.Z., Yan, M.J., 2011. Risk assessment of soil salinity by multiple-variable indicator kriging in the low plain around the Bohai Sea. Shuili Xuebao (J. Hydraul. Eng.) 42 (10), 1144–1151.
Zorer, O., Ceylan, H., Dogru, M., 2009. Determination of heavy metals and comparison to gross radioactivity concentration in soil and sediment samples of the Bendimahi river basin (Van, Turkey). Water Air Soil Pollut. 196 (1–4), 75–87.